Computers and Mathematics with Applications 59 (2010) 3516–3528

Contents lists available at ScienceDirect

Computers and Mathematics with Applications

journal homepage: www.elsevier.com/locate/camwa

Mixed convective heat and mass transfer in a vertical wavy channel with traveling thermal waves and porous medium

R. Muthuraj, S. Srinivas *

Fluid Dynamics Division, School of Advanced Sciences, VIT University, Vellore – 632 014, India

ARTICLE INFO

Article history:
Received 22 March 2009
Accepted 22 March 2010

Keywords:
Mixed convection
Wavy walls
Porous medium
Hartmann number
Sherwood number
Soret number

ABSTRACT

We investigate the problem of mixed convection heat and mass transfer through a vertical wavy channel with porous medium. The flow is generated by the periodic thermal waves prescribed at the wavy walls of the channel. The equations of momentum energy and concentration are solved subject to a set of appropriate boundary conditions by assuming that the solution consists of a mean part and a perturbed part. The effects of various pertinent parameters on flow, heat and mass transfer characteristics are discussed numerically and explained graphically.

1. Introduction

Many transport processes exist in nature and industrial applications in which the transfer of heat and mass occurs simultaneously as a result of combined buoyancy effects of thermal diffusion and diffusion of species. The engineering applications include the chemical distillatory processes, formation and dispersion of fog, design of heat exchangers, channel type solar energy collectors, and thermo-protection systems. Convection flows driven by temperature and concentration differences have been studied extensively in the past and various extensions of the problems have been reported in the literature (see for example [1,2] and several references therein). The study of viscous flows bounded by wavy wall is of special interest due to its application to transpiration cooling of re-entry vehicles and rocket booster, cross-hatching on ablative surfaces and film vaporization in combustion chambers. In view of these applications, Vajravelu [3] studied the combined free and forced convection in hydromagnetic flows in a vertical wavy channel with traveling thermal waves. Cho et al. [4] have studied the problem of linear stability of two-dimensional steady flow in wavy-walled channels. Chamka and Camille [5] have discussed the problem of mixed convection effects on unsteady flow and heat transfer over a stretched surface. They focused on the effects of mixed convection currents on the problem of unsteady, laminar, boundary layer flow and heat transfer of an electrically conducting and heat generating or absorbing fluid over a semi-infinite vertical stretched surface in the presence of a uniform magnetic field. Harris et al. [6] have numerically investigated the unsteady mixed convection boundary layer flow on a vertical surface in a porous medium. Barletta and Zanchini [7] investigated the study of time-periodic laminar mixed convection in an inclined channel with the temperature of one channel wall is stationary, while the temperature of the other wall is a sinusoidal function of time. Mebrouk et al. [8] have reported a numerical investigation of natural convection and fluid flow in a horizontal wavy enclosure. They consider the bottom wall is varied with a sinusoidal function while the top and the two side walls are flat. Eldabe et al. [9] have studied the problem of heat and mass transfer due to the steady motion of Rivlin–Ericksen fluid in tube of varying cross section. Jang and Yan [1] have discussed the study of mixed convection heat and mass transfer along a vertical wavy surface, which is maintained

* Corresponding author.
E-mail address: srinusuripeddi@hotmail.com (S. Srinivas).

0898-1221/$ – see front matter © 2010 Elsevier Ltd. All rights reserved.
doi:10.1016/j.camwa.2010.03.045

at uniform wall temperature and constant wall concentration. More recently, Eldabe et al. [2] discussed the problem of mixed convective heat and mass transfer in a non-Newtonian fluid at a peristaltic surface with temperature dependent viscosity. They considered the peristaltic flow is between two vertical walls, one of which is deformed in the shape of traveling transversal waves exactly like peristaltic pumping and the other of which is parallel flat plate wall.

The study of fluid flows and heat transfer through porous medium has attracted much attention recently. This is primarily because of numerous applications of flow through porous medium, such as storage of radioactive nuclear waste materials transfer, separation processes in chemical industries, filtration, transpiration cooling, transport processes in aquifers, ground water pollution, etc. Examples of natural porous media are beach sand, sandstone, limestone, rye bread, wood, the human lung, bile duct, gall bladder with stones and in small blood vessels. In some pathological situations, the distribution of fatty cholesterol and artery clogging blood clots in the lumen of coronary artery can be considered as equivalent to a porous medium. Comprehensive literature surveys concerning the subject of porous media can be found in the most recent books by Nield and Bejan [10], Vafai [11], Pop and Ingham [12], Bejan and Kraus [13]. Guria and Jana [14] studied hydrodynamic flow through vertical wavy channel with traveling thermal waves embedded in porous medium.

When heat and mass transfer occur simultaneously in a moving fluid, the relations between the fluxes and the driving potentials are of more intricate nature. It has been found that an energy flux can be generated not only by temperature gradients but by composition gradients as well. The energy flux caused by a composition gradient is called the Dufour or diffusion-thermo effect. On the other hand, mass fluxes can also be created by temperature gradients and this is the Soret or thermal-diffusion effect. In general, the thermal-diffusion and diffusion-thermo effects are of a smaller order of magnitude than the effects described by Fourier's or Fick's law and are often neglected in heat and mass transfer processes. However, exceptions are observed therein. Due to the importance of Soret (thermal-diffusion) and Dufour (diffusion-thermo) effects for the fluids with very light molecular weight as well as medium molecular weight many investigators have studied and reported interesting results for these flows [15–22]. To the best of the author's knowledge, the study of unsteady MHD flow of heat and mass transfer in a viscous fluid through the vertical wavy porous space with traveling thermal waves has not been studied. The objective of this study is to examine analytically the mixed convection heat and mass transfer in vertical wavy porous space with traveling thermal waves and thermal diffusion. Using long wave length approximation, the governing equations are solved by the perturbation technique for hydromagnetic case. The closed form solutions for velocity, temperature, skin friction, concentration, Nusselt number as well as Sherwood number are presented. The effects of pertinent parameters on flow and heat transfer characteristics are studied in detail.

2. Formulation of the problem

Consider the unsteady, combined convective heat and mass transfer, MHD flow of an electrically conducting viscous fluid confined to the vertical wavy walls embedded in a porous medium. We consider the wavy wall in which x axis is taken vertically upward, and parallel to the direction of buoyancy, and the y axis is normal to it. A uniform magnetic field is applied normal to the axial direction. The wavy walls are represented by $y = d + a\cos\lambda x$ and $y = -d + a\cos(\lambda x + \theta)$. The governing equations for this problem are based on the balance laws of mass, linear momentum and energy modified to account for the presence of the magnetic field, thermal buoyancy and heat generation or absorbing effects. These can be written as

$$\frac{\partial u}{\partial x} + \frac{\partial v}{\partial y} = 0 \tag{1}$$

$$\rho\left(\frac{\partial v}{\partial t} + u\frac{\partial v}{\partial x} + v\frac{\partial v}{\partial y}\right) = -\frac{\partial \rho}{\partial x} + \mu\left(\frac{\partial^2 v}{\partial x^2} + \frac{\partial^2 u}{\partial y^2}\right) - \frac{\mu}{k}u - \sigma B_0^2 u + \rho g\xi(T - T_1') + \rho g\xi^*(C - C_1') \tag{2}$$

$$\rho\left(\frac{\partial v}{\partial t} + u\frac{\partial v}{\partial x} + v\frac{\partial v}{\partial y}\right) = -\frac{\partial \rho}{\partial y} + \mu\left(\frac{\partial^2 v}{\partial x^2} + \frac{\partial^2 v}{\partial y^2}\right) - \frac{\mu}{k}v \tag{3}$$

$$\rho C_p\left(\frac{\partial T}{\partial t} + u\frac{\partial T}{\partial x} + v\frac{\partial T}{\partial y}\right) = K\left(\frac{\partial^2 T}{\partial x^2} + \frac{\partial^2 T}{\partial y^2}\right) + Q \tag{4}$$

$$\left(\frac{\partial C}{\partial t} + u\frac{\partial C}{\partial x} + v\frac{\partial C}{\partial y}\right) = D_m\left(\frac{\partial^2 C}{\partial x^2} + \frac{\partial^2 C}{\partial y^2}\right) + \frac{D_m k_T}{\overline{T}}\left(\frac{\partial^2 T}{\partial x^2} + \frac{\partial^2 T}{\partial y^2}\right). \tag{5}$$

The boundary conditions of the problem are

$$u = 0, \quad v = 0, \quad T = T_1', \quad C = C_1', \quad \text{at } y = d + a\cos\lambda x \tag{6}$$

$$u = 0, \quad v = 0, \quad T = T_2', \quad C = C_2', \quad \text{at } y = -d + a\cos(\lambda x + \theta) \tag{7}$$

where, $T_1\,[1 + \varepsilon\cos(\lambda x + \omega t)] = T_1', T_2\,[1 + \varepsilon\cos(\lambda x + \omega t)] = T_2', C_1\,[1 + \varepsilon\cos(\lambda x + \omega t)] = C_1', C_2\,[1 + \varepsilon\cos(\lambda x + \omega t)] = C_2'$, B_0 is the transverse magnetic field, D_m is the coefficient of mass diffusivity, p is the pressure, T is the temperature, $\lambda\ (=\lambda^*) = \lambda d$ is the non-dimensional wave number, λx is the wall wavinesss parameter, ρ is the density, ν is the kinematic viscosity, k is the permeability of the medium, σ is the coefficient of electric conductivity, ξ is the coefficient of thermal

expansion, ξ^* is the coefficient of expansion with concentration, ω-frequency parameter, β is the volumetric coefficient of thermal expansion, k_T is the thermal-diffusion ratio, T_1' and T_2' are the wall temperatures, C_1' and C_2' are the wall concentrations. $\overline{T}$ is the mean value of T_1' and T_2'.

We introduce the non-dimensional variables

$$(x^*, y^*) = \frac{1}{d}(x, y), \qquad t^* = \frac{t\nu}{d^2}, \qquad (u^*, v^*) = \frac{d}{\nu}(u, v), \qquad p^* = \frac{p}{\rho\left(\frac{\nu}{d}\right)^2},$$
$$T^* = \frac{T - T_1'}{T_2' - T_1'}, \qquad \phi = \frac{C - C_1'}{C_2' - C_1'}. \tag{8}$$

Invoking the above non-dimensional variables, the basic field equations (1)–(7) can be expressed in the non-dimensional form, dropping the asterisks,

$$\frac{\partial u}{\partial x} + \frac{\partial v}{\partial y} = 0 \tag{9}$$

$$\frac{\partial u}{\partial t} + u\frac{\partial u}{\partial x} + v\frac{\partial u}{\partial y} = -\frac{\partial p}{\partial x} + \left(\frac{\partial^2 u}{\partial x^2} + \frac{\partial^2 u}{\partial y^2}\right) - M^2 u - \frac{1}{D_a}u + G_c\phi + G_r T \tag{10}$$

$$\frac{\partial v}{\partial t} + u\frac{\partial v}{\partial x} + v\frac{\partial v}{\partial y} = -\frac{\partial p}{\partial y} + \left(\frac{\partial^2 v}{\partial x^2} + \frac{\partial^2 v}{\partial y^2}\right) - \frac{1}{D_a}v \tag{11}$$

$$\left(\frac{\partial T}{\partial t} + u\frac{\partial T}{\partial x} + v\frac{\partial T}{\partial y}\right) = \frac{1}{P_r}\left(\frac{\partial^2 T}{\partial x^2} + \frac{\partial^2 T}{\partial y^2}\right) + \alpha \tag{12}$$

$$\left(\frac{\partial \phi}{\partial t} + u\frac{\partial \phi}{\partial x} + v\frac{\partial \phi}{\partial y}\right) = \frac{1}{S_c}\left(\frac{\partial^2 \phi}{\partial x^2} + \frac{\partial^2 \phi}{\partial y^2}\right) + S_r\left(\frac{\partial^2 T}{\partial x^2} + \frac{\partial^2 T}{\partial y^2}\right) \tag{13}$$

$$u = 0, \qquad v = 0, \qquad T = 0, \qquad \phi = 0 \quad \text{at } y = 1 + \varepsilon\cos\lambda x \tag{14}$$

$$u = 0, \qquad v = 0, \qquad T = 1, \qquad \phi = 1 \quad \text{at } y = 1 + \varepsilon\cos(\lambda x + \theta) \tag{15}$$

where $G_r = d^3\xi g(T_2' - T_1')/\nu^2$ is the Grashof number $G_c = d^3\xi^* g(C_2' - C_1')/\nu^2$ is the local mass Grashof number, $M^2 = \sigma B_0^2 d^2/\rho\nu$ is the Hartmann number, $P_r = \mu C_p/K$ is the Prandtl number, $\nu = \mu/\rho$ is the kinematic viscosity, $\varepsilon = a/d$ is the non-dimensional amplitude parameter, $S_c = \mu/\rho D_m$ is the Schmidt number, $D_a = k/d^2$ is the porosity parameter, $\alpha = Qd^2/K(T_2' - T_1')$ is the heat source/sink parameter and $S_r = D_m k_T(T_2' - T_1')/\mu\overline{T}(C_2' - C_1')$ is the Soret number.

Let us introduce the stream function ψ defined by

$$u = -\frac{\partial \psi}{\partial y} \quad \text{and} \quad v = \frac{\partial \psi}{\partial x}. \tag{16}$$

Using Eq. (16), Eqs. (10)–(13) becomes

$$\frac{\partial^3\psi}{\partial x^2\partial t} + \frac{\partial^3\psi}{\partial y^2\partial t} - \frac{\partial\psi}{\partial y}\left(\frac{\partial^3\psi}{\partial x^3} + \frac{\partial^3\psi}{\partial x\partial y^2}\right) + \frac{\partial\psi}{\partial x}\left(\frac{\partial^3\psi}{\partial x^2\partial y} + \frac{\partial^3\psi}{\partial y^3}\right)$$
$$= \frac{\partial^4\psi}{\partial x^4} + 2\frac{\partial^4\psi}{\partial x^2\partial y^2} + \frac{\partial^4\psi}{\partial y^4} - M^2\frac{\partial^2\psi}{\partial y^2} - \frac{1}{D_a}\left(\frac{\partial^2\psi}{\partial x^2} + \frac{\partial^2\psi}{\partial y^2}\right) - G_r\frac{\partial T}{\partial y} - G_c\frac{\partial\phi}{\partial y} \tag{17}$$

$$\frac{\partial T}{\partial t} - \frac{\partial\psi}{\partial y}\frac{\partial T}{\partial x} + \frac{\partial\psi}{\partial x}\frac{\partial T}{\partial y} = \frac{1}{P_r}\left(\frac{\partial^2 T}{\partial x^2} + \frac{\partial^2 T}{\partial y^2}\right) + \alpha \tag{18}$$

$$\frac{\partial\phi}{\partial t} - \frac{\partial\psi}{\partial y}\frac{\partial\phi}{\partial x} + \frac{\partial\psi}{\partial x}\frac{\partial\phi}{\partial y} = \frac{1}{S_c}\left(\frac{\partial^2\phi}{\partial x^2} + \frac{\partial^2\phi}{\partial y^2}\right) + S_r\left(\frac{\partial^2 T}{\partial x^2} + \frac{\partial^2 T}{\partial y^2}\right). \tag{19}$$

The boundary conditions (14) and (15) become

$$\psi_y = \psi_x = 0, \qquad T = 0, \qquad \phi = 0 \quad \text{at } y = 1 + \varepsilon\cos\lambda x \tag{20}$$

$$\psi_y = \psi_x = 0, \qquad T = 1, \qquad \phi = 1 \quad \text{at } y = -1 + \varepsilon\cos(\lambda x + \theta). \tag{21}$$

3. Solution of the problem

In order to solve Eqs. (17)–(19) we assume that the solution consists of a mean part and a perturbed part so that the stream function, temperature and concentration distributions are

$$\psi(x,y,t) = \psi_0(y) + \psi_1(x,y,t) \tag{22}$$
$$T(x,y,t) = T_0(y) + T_1(x,y,t) \tag{23}$$
$$\phi(x,y,t) = \phi_0(y) + \phi_1(x,y,t) \tag{24}$$

where ψ_0, T_0, ϕ_0 are the mean parts and ψ_1, T_1, ϕ_1 are the perturbed parts also, we introduce

$$\psi_1(x,y,t) = \varepsilon\, \mathrm{e}^{\mathrm{i}(\lambda x+\omega t)}\bar{\psi}_1(y) \tag{25}$$
$$T_1(x,y,t) = \varepsilon\, \mathrm{e}^{\mathrm{i}(\lambda x+\omega t)}\bar{T}_1(y) \tag{26}$$
$$\phi_1(x,y,t) = \varepsilon\, \mathrm{e}^{\mathrm{i}(\lambda x+\omega t)}\bar{\phi}_1(y) \tag{27}$$

with the help of Eqs. (22)–(27) the Eqs. (17)–(21) yield

$$\psi_0^{iv} - \left(M^2 + \frac{1}{D_a}\right)\psi_0'' - G_r T_0' - G_c\phi_0' = 0 \tag{28}$$
$$T_0'' + \alpha = 0 \tag{29}$$
$$\phi_0'' + S_r S_c T_0'' = 0 \tag{30}$$

together with the boundary conditions

$$\psi_0' = 0, \quad \psi_0 = 0, \quad T_0 = 0, \quad \phi_0 = 0 \quad \text{at } y = 1 \tag{31}$$
$$\psi_0' = 0, \quad \psi_0 = 0, \quad T_0 = 1, \quad \phi_0 = 1 \quad \text{at } y = -1 \tag{32}$$

to the zeroth order, and

$$\bar{\psi}_1^{iv} - \mathrm{i}\omega(\bar{\psi}_1'' - \lambda^2\bar{\psi}_1) + \mathrm{i}\lambda\psi_0'(\bar{\psi}_1'' - \lambda^2\bar{\psi}_1) - \mathrm{i}\lambda\bar{\psi}_1\psi_0''' - 2\lambda^2\bar{\psi}_1'' + \lambda^4\bar{\psi}_1 - M^2\bar{\psi}_1'' - \frac{1}{D_a}(\bar{\psi}_1'' - \lambda^2\bar{\psi}_1) - G_r\bar{T}_1' - G_c\overline{\phi}_1' = 0 \tag{33}$$
$$\bar{T}_1'' - \mathrm{i}P_r\omega\bar{T}_1' + \mathrm{i}P_r\lambda(\psi_0'\bar{T}_1 - \bar{\psi}_1 T_0') - \lambda^2\bar{T}_1 = 0 \tag{34}$$
$$\overline{\phi}_1'' - \mathrm{i}S_c\omega\overline{\phi}_1' + \mathrm{i}S_c\lambda(\psi_0'\overline{\phi}_1 - \bar{\psi}_1 T_0') - \lambda^2\overline{\phi}_1 = 0 \tag{35}$$

together with the boundary conditions

$$\bar{\psi}_1' = -\psi_0''\mathrm{e}^{-\mathrm{i}\omega t}, \quad \bar{\psi}_1 = 0, \quad \bar{T}_1 = -\mathrm{e}^{-\mathrm{i}\omega t}T_0', \quad \overline{\phi}_1 = -\mathrm{e}^{-\mathrm{i}\omega t}\phi_0' \quad \text{at } y = 1 \tag{36}$$
$$\bar{\psi}_1' = -\psi_0''\mathrm{e}^{\mathrm{i}(\theta-\omega t)}, \quad \bar{\psi}_1 = 0, \quad \bar{T}_1 = -\mathrm{e}^{\mathrm{i}(\theta-\omega t)}T_0', \quad \overline{\phi}_1 = -\mathrm{e}^{\mathrm{i}(\theta-\omega t)}\phi_0' \quad \text{at } y = -1 \tag{37}$$

to the first order, where a prime denotes differentiation with respect to y.

For small values of λ, we can expand $\bar{\psi}_1$, $\bar{T}_1$ and $\overline{\phi}_1$ in terms of λ so that

$$\bar{\psi}_1(\lambda,y) = \sum_{r=0}^{\infty}\lambda^r\bar{\psi}_{1r}, \quad \bar{T}_1(\lambda,y) = \sum_{r=0}^{\infty}\lambda^r\bar{T}_{1r}, \quad \overline{\phi}_1(\lambda,y) = \sum_{r=0}^{\infty}\lambda^r\overline{\phi}_{1r}. \tag{38}$$

Substituting (38) into (33)–(37), we get the following sets of ordinary differential equations and the boundary conditions, to the order of λ:

$$\bar{\psi}_{10}^{iv} - \mathrm{i}\omega\bar{\psi}_{10}'' - \left(M^2 + \frac{1}{D_a}\right)\psi_{10}'' - G_r\bar{T}_{10}' - G_c\overline{\phi}_{10}' = 0 \tag{39}$$
$$\bar{T}_{10}'' - P_r\mathrm{i}\omega\bar{T}_{10}' = 0 \tag{40}$$
$$\overline{\phi}_{10}'' - S_c\mathrm{i}\omega\overline{\phi}_{10}' = 0 \tag{41}$$
$$\bar{\psi}_{11}^{iv} - \mathrm{i}\omega\bar{\psi}_{11}'' + \mathrm{i}(\psi_0'\bar{\psi}_{10}'' - \bar{\psi}_{10}\psi_0''') - \left(M^2 + \frac{1}{D_a}\right)\bar{\psi}_{11}'' - G_r\bar{T}_{11}' - G_c\overline{\phi}_{11}' = 0 \tag{42}$$
$$\bar{T}_{11}'' - P_r\mathrm{i}\omega\bar{T}_{11}^{+}P_r\mathrm{i}(\psi_0'\bar{T}_{10} - \bar{\psi}_{10}T_0') = 0 \tag{43}$$
$$\overline{\phi}_{11}'' - S_c\mathrm{i}\omega\overline{\phi}_{11}^{+}S_c\mathrm{i}(\psi_0'\overline{\phi}_{10} - \bar{\psi}_{10}\phi_0') = 0 \tag{44}$$
$$\bar{\psi}_{10}' = -\psi_0''\mathrm{e}^{-\mathrm{i}\omega t}, \quad \bar{\psi}_{10} = 0, \quad \bar{T}_{10} = -\mathrm{e}^{-\mathrm{i}\omega t}T_0', \quad \overline{\phi}_{10} = -\mathrm{e}^{-\mathrm{i}\omega t}\phi_0' \quad \text{at } y = 1 \tag{45}$$
$$\bar{\psi}_{10}' = -\psi_0''\mathrm{e}^{\mathrm{i}(\theta-\omega t)}, \quad \bar{\psi}_{10} = 0, \quad \bar{T}_{10} = -\mathrm{e}^{\mathrm{i}(\theta-\omega t)}T_0', \quad \overline{\phi}_{10} = -\mathrm{e}^{\mathrm{i}(\theta-\omega t)}\phi_0' \quad \text{at } y = -1 \tag{46}$$
$$\left.\begin{array}{l}\bar{\psi}_{1r}' = 0, \quad \bar{\psi}_{1r} = 0 \quad \bar{T}_{1r} = 0, \quad \overline{\phi}_{1r} = 0, \quad \text{at } y = 1\\ \bar{\psi}_{1r}' = 0, \quad \bar{\psi}_{1r} = 0 \quad \bar{T}_{1r} = 0, \quad \overline{\phi}_{1r} = 0, \quad \text{at } y = -1\end{array}\right\} r \geq 1. \tag{47}$$

3.1. Zeroth-order solution

The solution of Eqs. (28)–(30) subject to the boundary conditions (31) and (32) are

$$\psi_0(y) = A_1(y^3+1) + A_2(y^2-1) + A_3(y+1) + A_4(e^{\beta y} - e^{-\beta}) + A_5(e^{\beta} - e^{-\beta y})$$
$$T_0(y) = -\left(\frac{\alpha}{2}\right)y^2 - \left(\frac{1}{2}\right)y + \frac{1}{2}(\alpha+1)$$
$$\phi_0(y) = \left(\frac{\alpha S_c S_r}{2}\right)y^2 - \left(\frac{1}{2}\right)y + \frac{1}{2}(1-\alpha S_c S_r)$$

where

$$\beta = \sqrt{M^2 + \frac{1}{D_a}}; \qquad A_1 = \left(\frac{G_r\alpha - G_c S_c S_r \alpha}{6\beta^2}\right); \qquad A_2 = \left(\frac{G_r + G_c}{4\beta^2}\right);$$
$$A_3 = \left(\frac{G_c S_c S_r \alpha - G_r\alpha}{6\beta^2} - \frac{\alpha\sinh\beta(G_r - G_c S_c S_r)}{3\beta^2(\sinh\beta - \beta\cosh\beta)}\right); \qquad A_4 = \left(\frac{\alpha(G_r - G_c S_c S_r)}{6\beta^2(\sinh\beta - \beta\cosh\beta)} - \frac{G_r + G_c}{4\beta^3\sinh\beta}\right),$$
$$A_5 = \left(\frac{\alpha(G_r - G_c S_c S_r)}{6\beta^2(\sinh\beta - \beta\cosh\beta)} + \frac{G_r + G_c}{4\beta^3\sinh\beta}\right).$$

3.2. First-order solution

The solutions of Eqs. (39) and (41), subject to the conditions (45) and (46) are

$$\begin{aligned}\bar{\psi}_{10} &= B_1 + B_3 y\sinh N + B_5 e^{Ny} - B_7 e^{-Ny} + [6A_1 y + 2A_2 + \beta^2(A_4 e^{\beta y} - A_5 e^{-\beta y})] \\ &\quad \times (B_2 + B_4 y\sinh N + B_6 e^{Ny} - B_8 e^{-Ny})[(y\beta_1 - 2)B_9 + B_{10}]e^{\beta_1 y} \\ &\quad + [B_{11} - B_{12}(y\beta_1 - 2)]e^{-\beta_1 y} + [(y\beta_2 - 2)B_{13} + B_{14}]e^{\beta_2 y} + [B_{15} - B_{16}(y\beta_2 - 2)]e^{-\beta_2 y}\end{aligned}$$
$$\overline{T}_{10} = (\alpha y + 1/2)[S_4 e^{\beta_1 y} + S_5 e^{-\beta_1 y}]$$
$$\overline{\phi}_{10} = B_{17}(e^{\beta_2 y} - e^{-\beta_2 y}) + \phi_0'(y)(B_{18}e^{\beta_2 y} - B_{19}e^{-\beta_2 y}) - B_{20}e^{\beta_1 y} + B_{21}e^{-\beta_1 y} - B_{22}y - B_{23}$$

where,

$$B_1 = \frac{S_{33}+S_{34}}{2} + \left[\frac{(S_{38}S_{39} - S_{37}S_{40})e^N - (S_{37}S_{39} - S_{38}S_{40})e^{-N} - \sinh N(S_{39} - S_{40})(S_{37} + S_{38})}{S_{37}^2 - S_{38}^2}\right]$$
$$B_2 = \left[\frac{[(e^{i\theta} - 1)(S_{37} + S_{38})\sinh N - (S_{38}e^{i\theta} - S_{37}) + (S_{37}e^{i\theta} - S_{38})]\cos\omega t}{S_{37}^2 - S_{38}^2}\right]$$
$$B_3 = \frac{S_{33} - S_{34}}{2} - \left[\frac{(S_{37} + S_{38})(S_{39} - S_{40})}{S_{37}^2 - S_{38}^2}\right]\sinh N; \qquad B_4 = \frac{e^{i\theta} - 1}{S_{37} - S_{38}}; \qquad B_5 = \frac{S_{37}S_{39} - S_{38}S_{40}}{S_{37}^2 - S_{38}^2};$$
$$B_6 = \frac{\cos\omega t(S_{38}e^{i\theta} - S_{37})}{S_{37}^2 - S_{38}^2}; \qquad B_7 = \frac{S_{38}S_{39} - S_{37}S_{40}}{S_{37}^2 - S_{38}^2}; \qquad B_8 = \frac{\cos\omega t(S_{37}e^{i\theta} - S_{38})}{S_{37}^2 - S_{38}^2}; \qquad B_9 = S_4 S_{21} S_{27};$$
$$B_{10} = S_{22}S_{31} - S_4 S_{21} S_{28}; \qquad B_{11} = S_{23}S_{31} - S_5 S_{21} S_{28}; \qquad B_{12} = S_5 S_{21} S_{27}; \qquad B_{13} = S_{19}S_{26}S_{29}; \qquad B_{16} = S_{20}S_{26}S_{29};$$
$$B_{14} = S_{24}S_{32} - S_{19}S_{26}S_{30}; \qquad B_{15} = S_{15}S_{32} - S_{20}S_{26}S_{30}; \qquad B_{17} = \frac{S_{10}e^{\beta_2} - S_{11}e^{-\beta_2}}{2\sinh(2\beta_2)}; \qquad B_{18} = \frac{S_{12}\cos\omega t}{2\sinh(2\beta_2)};$$
$$B_{19} = \frac{S_{13}\cos\omega t}{2\sinh(2\beta_2)}; \qquad B_{20} = S_4(S_8 + S_9); \qquad B_{21} = S_5(S_9 - S_8); \qquad B_{22} = S_6(S_4 + S_5); \qquad B_{23} = S_6 S_7(S_5 - S_4)$$
$$\beta_1 = \sqrt{iP_r\omega}; \qquad \beta_2 = \sqrt{iS_c\omega}; \qquad N = \sqrt{i\omega + \frac{1}{D_a} + M^2}; \qquad S_1 = -\frac{\cos\omega t}{2\sinh(2\beta_1)}; \qquad S_2 = e^{i\theta}e^{-\beta_1} - e^{\beta_1};$$
$$S_3 = e^{-\beta_1} - e^{i\theta}e^{\beta_1}; \qquad S_4 = S_1 S_2; \qquad S_5 = S_1 S_3; \qquad S_6 = \frac{S_r S_c \alpha\beta_1^2}{\beta_1^2 - \beta_2^2}; \qquad S_7 = \frac{2\beta_1}{\beta_1^2 - \beta_2^2}; \qquad S_8 = \frac{S_r S_c \beta_1^2}{2(\beta_1^2 - \beta_2^2)};$$
$$S_9 = \frac{2\alpha S_r S_c \beta_1}{\beta_1^2 - \beta_2^2}; \qquad S_{10} = B_{20}e^{\beta_1} - B_{21}e^{-\beta_1} + B_{22} + B_{23}; \qquad S_{11} = B_{20}e^{-\beta_1} - B_{21}e^{\beta_1 y} - B_{22} + B_{23};$$
$$S_{12} = e^{i\theta}e^{-\beta_2} - e^{\beta_2}; \qquad S_{13} = e^{i\theta}e^{\beta_2} - e^{-\beta_2}; \qquad S_{14} = \frac{S_{10}e^{\beta_2} - S_{11}e^{-\beta_2} + S_{12}\cos\omega t}{2\sinh(2\beta_2)};$$

$$S_{15} = \frac{S_{10}e^{\beta_2} - S_{11}e^{-\beta_2} - S_{13}\cos\omega t}{2\sinh(2\beta_2)}; \qquad S_{16} = S_6(S_4 + S_5); \qquad S_{17} = S_4(S_8 + S_9); \qquad S_{18} = S_5(S_9 - S_8);$$

$$S_{19} = \frac{S_{12}\cos\omega t}{2\sinh(2\beta_2)}; \qquad S_{20} = \frac{S_{13}\cos\omega t}{2\sinh(2\beta_2)}; \qquad S_{21} = G_r\alpha\beta_1; \qquad S_{22} = \frac{G_r\beta_1 S_4}{2} + G_r\alpha S_4 - G_c\beta_1 S_{17};$$

$$S_{23} = -\frac{G_r\beta_1 S_5}{2} + G_r\alpha S_5 - G_c\beta_1 S_{18}; \qquad S_{24} = G_c\alpha S_c S_r S_{19} - G_c\beta_2 S_{14} - \frac{G_c\beta_2 S_{19}}{2};$$

$$S_{25} = G_c\alpha S_c S_r S_{19} + G_c\beta_2 S_{15} + G_c\beta_2 S_{20}; \qquad S_{26} = G_r\alpha\beta_2 S_c S_r; \qquad S_{27} = \frac{1}{\beta_1^3(\beta_1^2 - N^2)}; \qquad S_{28} = \frac{2}{\beta_1(\beta_1^2 - N^2)^2};$$

$$S_{29} = \frac{1}{\beta_2^3(\beta_2^2 - N^2)}; \qquad S_{30} = \frac{2}{\beta_2(\beta_2^2 - N^2)^2}; \qquad S_{31} = \frac{1}{\beta_1^4 - N^2\beta_1^2}; \qquad S_{32} = \frac{1}{\beta_2^4 - N^2\beta_2^2};$$

$$\begin{aligned} S_{33} &= B_1 + B_3\sinh N + B_5 e^N - B_7 e^{-N} + [(\beta_1 - 2)B_9 + B_{10}]e^{\beta_1} + [B_{11} - B_{12}(\beta_1 - 2)]e^{-\beta_1} \\ &\quad + [(\beta_2 - 2)B_{13} + B_{14}]e^{\beta_2} + [B_{15} - B_{16}(\beta_2 - 2)]e^{-\beta_2} \\ S_{34} &= B_1 - B_3\sinh N + B_5 e^{-N} - B_7 e^N + [B_{10} - (\beta_1 + 2)B_9]e^{-\beta_1} + [B_{11} + B_{12}(\beta_1 + 2)]e^{\beta_1} \\ &\quad + [B_{14} - (\beta_2 + 2)B_{13}]e^{-\beta_2} + [B_{15} + B_{16}(\beta_2 + 2)]e^{\beta_2} \\ S_{35} &= B_3\sinh N + N(B_5 e^N + B_7 e^{-N}) + [(\beta_1 - 2)B_9 + B_{10}]\beta_1 e^{\beta_1} - \beta_1[B_{11} - B_{12}(\beta_1 - 2)]e^{-\beta_1} \\ &\quad + [(\beta_2 - 2)B_{13} + B_{14}]\beta_2 e^{\beta_2} - \beta_2[B_{15} - B_{16}(\beta_2 - 2)]e^{-\beta_2} + \beta_1 B_9 e^{\beta_1} - \beta_1 B_{12} e^{-\beta_1} + \beta_2 B_{13} e^{\beta_2} - \beta_2 B_{16} e^{-\beta_2} \\ S_{36} &= B_3\sinh N + N(B_5 e^{-N} + B_7 e^N) - [(\beta_1 + 2)B_9 - B_{10}]\beta_1 e^{-\beta_1} - \beta_1[B_{11} + B_{12}(\beta_1 + 2)]e^{\beta_1} \\ &\quad - [(\beta_2 + 2)B_{13} - B_{14}]\beta_2 e^{-\beta_2} - \beta_2[B_{15} + B_{16}(\beta_2 + 2)]e^{\beta_2} + \beta_1 B_9 e^{-\beta_1} - \beta_1 B_{12} e^{\beta_1} + \beta_2 B_{13} e^{-\beta_2} - \beta_2 B_{16} e^{\beta_2} \end{aligned}$$

$$S_{37} = [Ne^N - \sinh N]; \qquad S_{38} = [\sinh N - Ne^{-N}]; \qquad S_{39} = \frac{2S_{35} - S_{33} + S_{34}}{2}; \qquad S_{40} = \frac{S_{33} - S_{34} - 2S_{36}}{2}.$$

We can evaluate the main flow velocity and the cross velocity by integrating from Eq. (16).

The shear stress at any point in the fluid is given by

$$\bar{\tau}_{xy} = \mu\left(\frac{\partial u}{\partial y} + \frac{\partial v}{\partial x}\right). \tag{48}$$

In non-dimensionless form

$$\tau = \left(\frac{d^2}{\rho\nu^2}\right)\bar{\tau}_{xy} = \frac{\partial u}{\partial y} + \frac{\partial v}{\partial x}. \tag{49}$$

At the wavy walls $y = 1 + \varepsilon\cos\lambda x$ and $y = -1 + \varepsilon\cos(\lambda x + \theta)$, the skin friction τ_{xy} becomes

$$\tau_1 = \tau_1^0 - \varepsilon\, Re[e^{i\lambda x}\psi_0'''(1) + e^{i(\lambda x+\omega t)}\overline{\psi}_1''(1)] \tag{50}$$

$$\tau_2 = \tau_2^0 - \varepsilon\, Re[e^{i\lambda x+\theta}\psi_0'''(-1) + e^{i(\lambda x+\omega t)}\overline{\psi}_1''(-1)] \tag{51}$$

respectively, where

$$\tau_1^0 = -\psi_0''(1); \qquad \tau_2^0 = -\psi_0''(-1). \tag{52}$$

The heat transfer coefficient, characterized by Nusselt number (Nu) on the tube boundary is

$$h = -K\frac{\partial T}{\partial y}. \tag{53}$$

In dimensionless form it becomes,

$$h = -K\left(\frac{T_2 - T_1}{d}\right)\left[T_0'(y) + \varepsilon\,[Re\; e^{i(\lambda x+\omega t)}\overline{T}_1'(y)]\right]. \tag{54}$$

At the wavy walls $y = 1 + \varepsilon\cos\lambda x$ and $y = -1 + \varepsilon\cos(\lambda x + \theta)$ the Nusselt number becomes

$$Nu_1 = Nu_1^0 + \varepsilon\, Re[e^{i\lambda x}T_0''(1) + e^{i(\lambda x+\omega t)}\overline{T}_1'(1)] \tag{55}$$

$$Nu_2 = Nu_2^0 + \varepsilon\, Re[e^{i(\lambda x+\theta)}T_0''(-1) + e^{i(\lambda x+\omega t)}\overline{T}_1'(-1)] \tag{56}$$

respectively, where

$$Nu_1^0 = T_0'(1); \qquad Nu_2^0 = T_0'(-1). \tag{57}$$

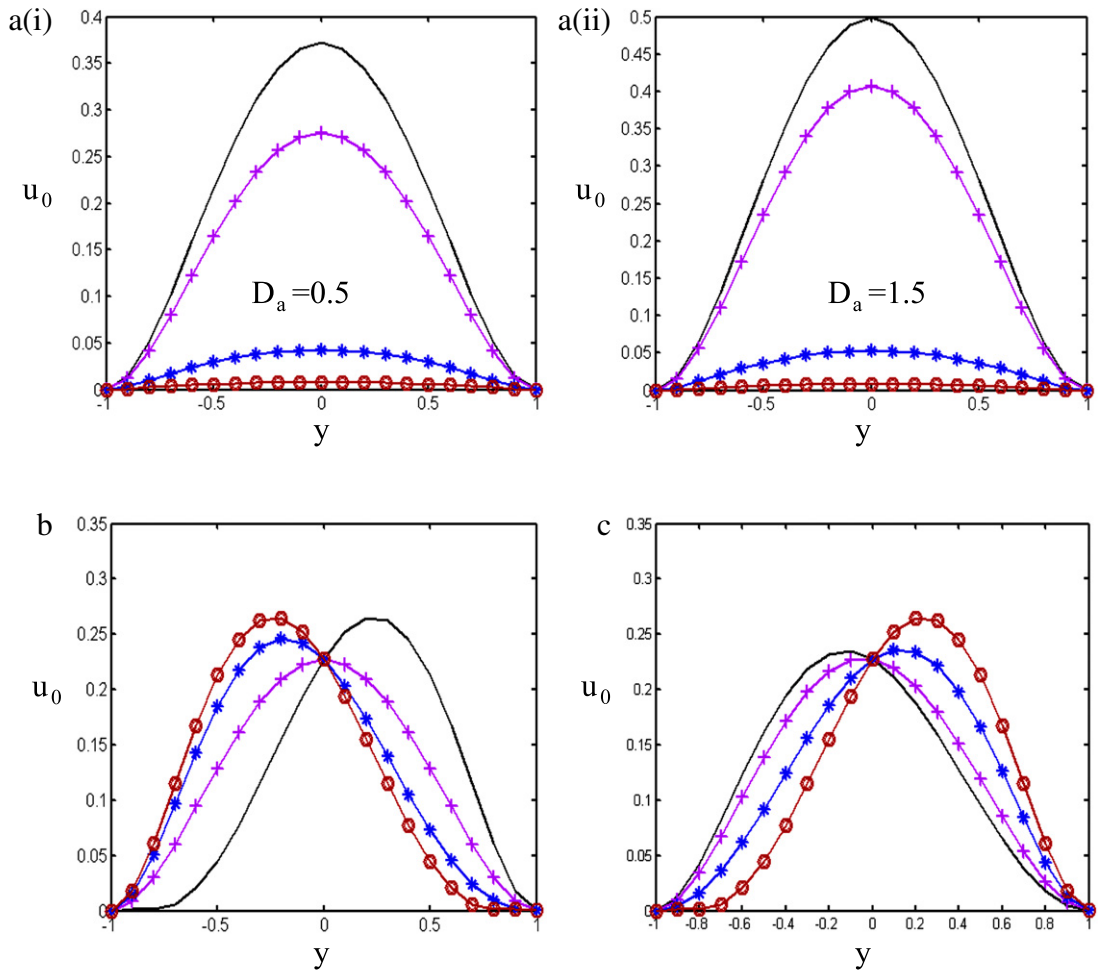

Fig. 1. Effect of M, D_a, α, S_c on zeroth-order velocity distribution. (a) $-M = 0, + M = 2, * M = 4, \circ M = 6, \alpha = 0.5, S_c = 0.5$. (b) $-\alpha = -3, + \alpha = 0, * \alpha = 2, \circ \alpha = 3, S_c = 0.5, M = 2, D_a = 0.5$. (c) $-S_c = 0, + S_c = 1, * S_c = 3, \circ S_c = 5, M = 2, D_a = 0.5, \alpha = 0.5$.

The dimensionless mass transfer number corresponding to the Nusselt number is the Sherwood number, written as,

$$Sh = \frac{\partial \phi}{\partial y}. \tag{58}$$

At the wavy walls $y = 1 + \varepsilon \cos \lambda x$ and $y = -1 + \varepsilon \cos(\lambda x + \theta)$, Sherwood number becomes

$$Sh_1 = Sh_1^0 + \varepsilon\, Re[e^{i\lambda x}\phi_0''(1) + e^{i(\lambda x+\omega t)}\overline{\phi}_1'(1)] \tag{59}$$

$$Sh_2 = Sh_2^0 + \varepsilon\, Re[e^{i(\lambda x+\theta)}\phi_0''(-1) + e^{i(\lambda x+\omega t)}\overline{\phi}_1'(-1)] \tag{60}$$

respectively, where

$$Sh_1^0 = \phi_0'(1), \qquad Sh_2^0 = \phi_0'(-1) \quad \text{and} \quad Re\text{-denotes real part.} \tag{61}$$

4. Results and discussions

To study the behavior of solutions, numerical calculations for several values of Hartmann number (M), frequency parameter (ω), Porosity parameter (D_a), Prandtl number (P_r), and Grashof number (G_r), local mass Grashof number (G_c), heat source/sink parameter (α), Soret number (S_r), and Schmidt number (S_c) have been carried out. The non-dimensional zeroth-order velocity u_0 is presented for different values of the parameters M, D_a, α, S_c with fixed values of $G_c = 15, G_r = 10, \lambda x = \pi/2, S_r = 0.5, \omega = 5, P_r = 0.73, \theta = 0$ in Fig. 1. Fig. 1(a) shows that u_0 decreases with the increase of M. The effect of D_a on u_0 is quite opposite to that of M. Fig. 1(b) illustrates the influence of α on u_0. We notice that there is an increase in the velocity u_0 with the increasing values of α in the first half of the channel while the reverse effect could be noticed in

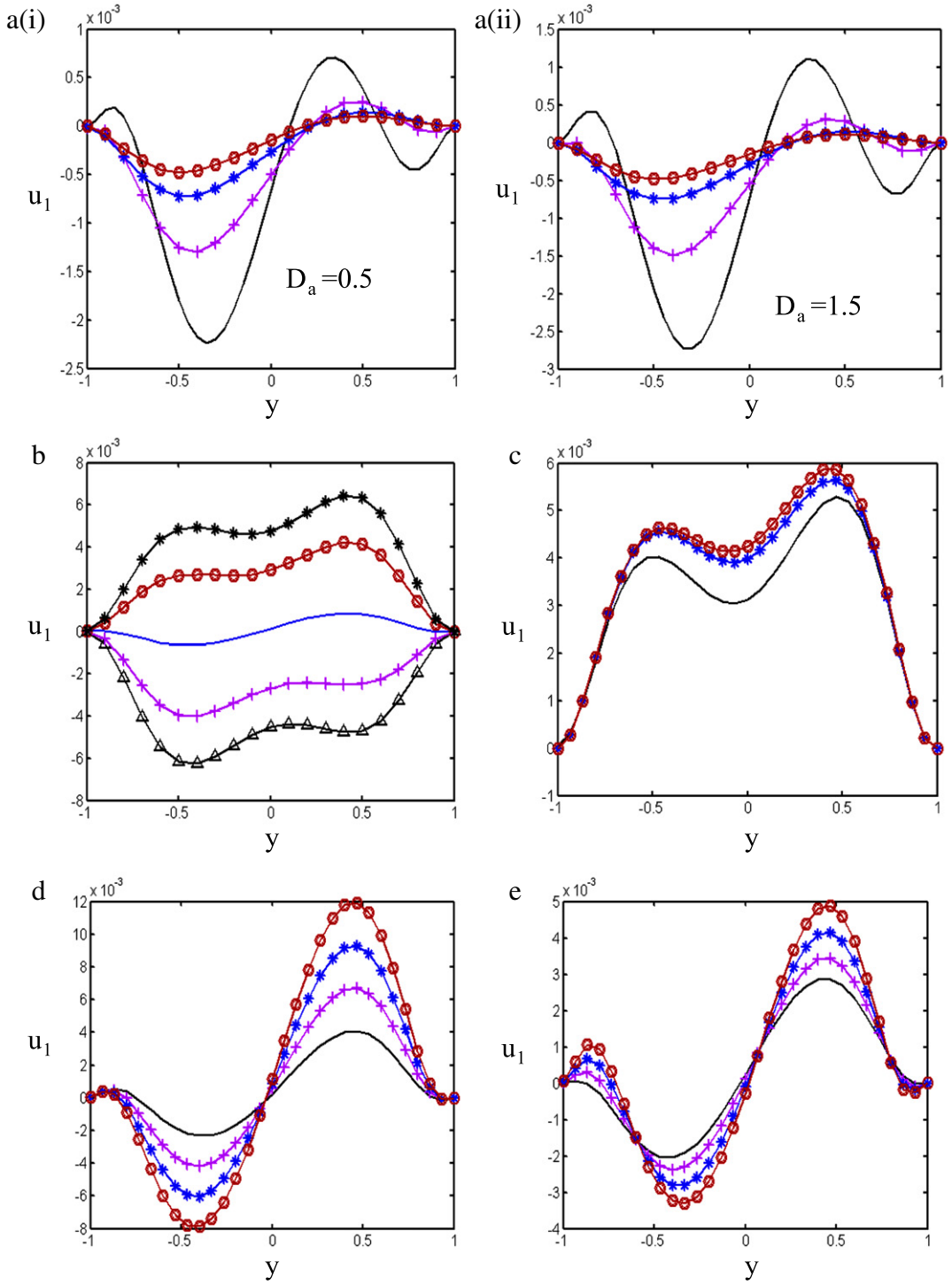

Fig. 2. Effect of M, D_a, α, S_c, G_r, G_c on first-order velocity distribution. (a) $-M = 0, +M = 2, *M = 4, \circ M = 6, G_r = 15, G_c = 10, S_c = 0.5, S_r = 0.5\alpha = -0.5$. (b) $-\alpha = -3, +\alpha = 2, \alpha = 0 \circ \alpha = 2, *\alpha = 3, G_r = 15, G_c = 10, D_a = 0.5, S_c = 0.5, S_r = 0.5, M = 2$. (c) $-S_c = 1, *S_c = 3, \circ S_c = 5, S_c = 5, G_r = 15, G_c = 10, S_c = 0.5, D_a = 0.5, M = 2, \alpha = 0.5$. (d) $-G_r = 5, +G_r = 10, *G_r = 15, \circ G_r = 20, G_c = 10, S_r = 0.5, D_a = 0.5, S_c = 0.5, M = 2, \alpha = 0.5$. (e) $-G_c = 1, +G_c = 5, *G_c = 10, \circ G_c = 15, G_r = 15, S_r = 0.5, S_c = 0.5, D_a = 0.5, M = 2, \alpha = 0.5$.

the other half of the channel. The opposite effect can be noticed in Fig. 1(c) if α is replaced by S_c. From these figures, one can observe that the fluid velocity u_0 is affected significantly by an increase in the parameters M, D_a, α, S_c. We note that u_0 increases by increasing y up to a maximum value (at a constant value of y) after which it decreases as noted in Ref. [2].

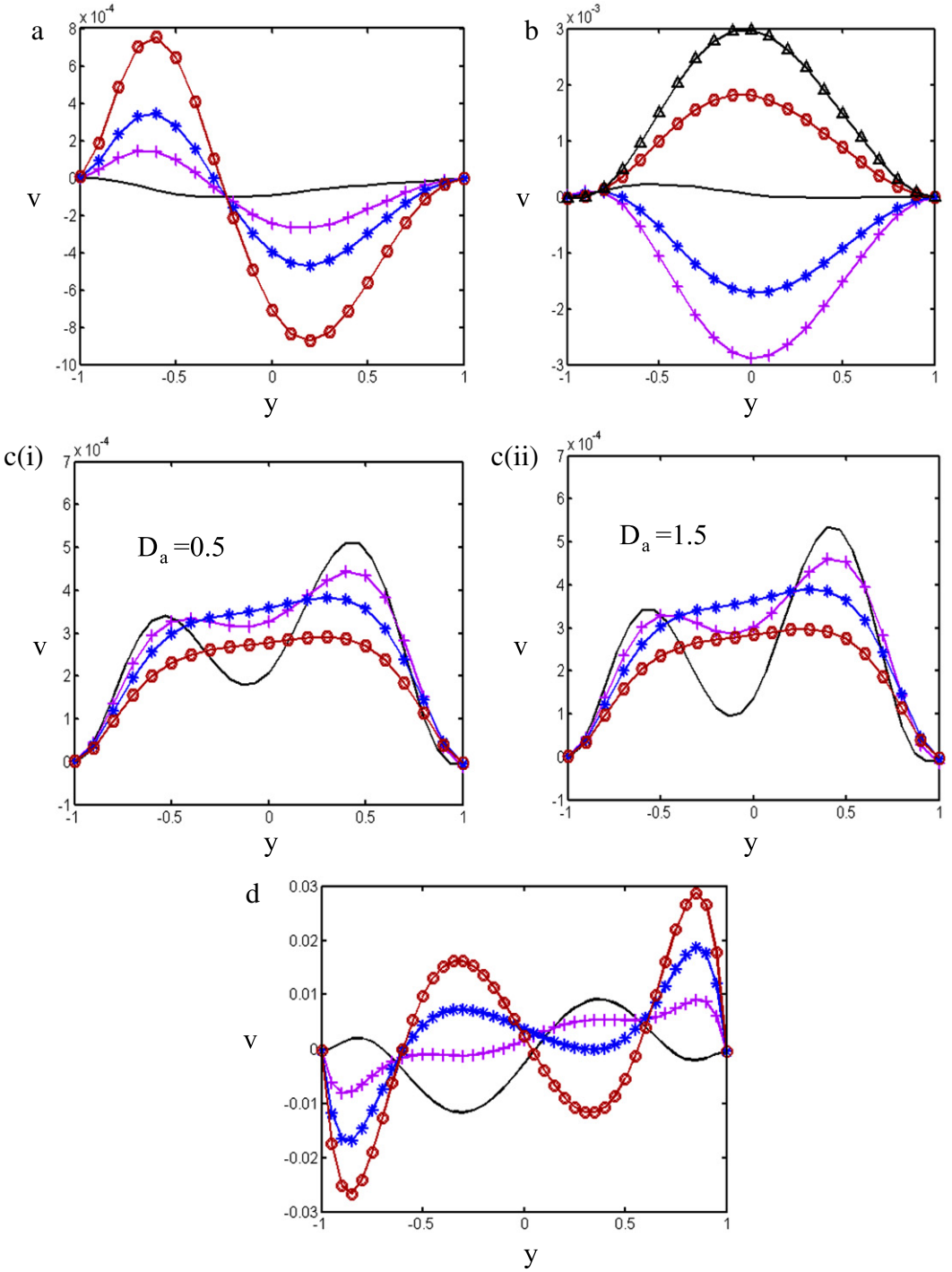

Fig. 3. Effect of $S_r, \alpha, M, D_a, \theta$ on cross velocity distribution. (a) $-S_r = 0, + S_r = 0.5, * S_r = 1, \circ S_r = 1.5, G_c = 10, G_r = 15, S_c = 0.5, M = 2, \alpha = 0.5, \theta = 0, D_a = 0.5$. (b) $-\alpha = 0, * \alpha = -3, + \alpha = -5, \circ \alpha = 3, \wedge \alpha = 5, G_c = 10, G_r = 15, S_r = 0.05, S_c = 0.05, M = 2, \theta = 0, D_a = 0.5$. (c) $-M = 0, + M = -0.5, * M = 1, \circ M = 1.5, G_c = 10, G_r = 15, S_r = 0.05, S_c = 0.05, \theta = 0$. (d) $-\theta = 0, + \theta = \pi/8, * \theta = \pi/4, \circ \theta = \pi/2, G_c = 10, G_r = 15, S_r = 0.05, S_c = 0.05, M = 2, D_a = 0.5$.

The effects of M, D_a, S_c, G_r, G_c and α on first-order velocity distribution u_1 are plotted in Fig. 2 with fixed values of $\lambda x = \pi/2$, $S_r = 0.5$, $\omega = 10$, $P_r = 0.73$, $\varepsilon = 0.02$ and $\theta = 0$. Fig. 2(a) depicts the behavior of perturbed quantity u_1 as a function of y when $D_a = 0.5$ and 1.5. On fixing D_a and changing M, we notice from the Fig. 2(a)(i) that the profiles exhibit the sharp decrease near the wavy wall as well as its moderate enhancement occurs in the central part of the channel. Further, from Fig. 2(a)(i) and (a)(ii), amplitude of u_1 increases by increasing D_a. It may also be noticed that u_1 remains negative in

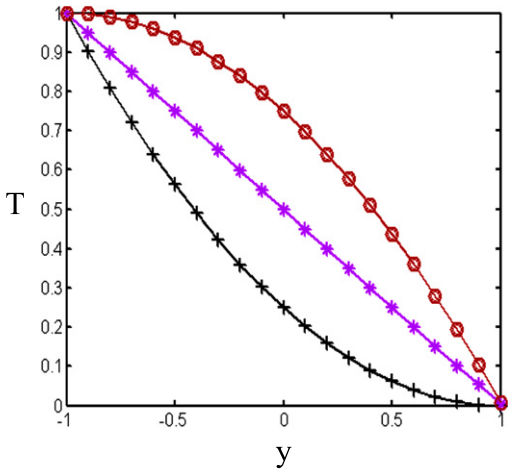

Fig. 4. Temperature distribution $+\ \alpha = -0.5, *\ \alpha = 0, \circ\ \alpha = 0.5$.

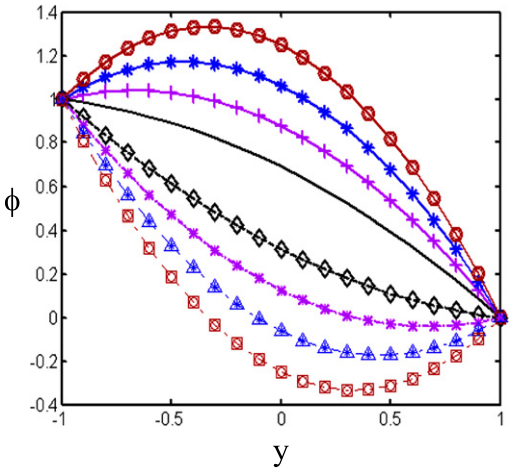

Fig. 5. Concentration distribution. $-S_c = 0.5, +S_c = 1, *S_c = 1.5, \circ S_c = 2, \alpha = -0.5$ and $\ldots\ \alpha = 0.5$.

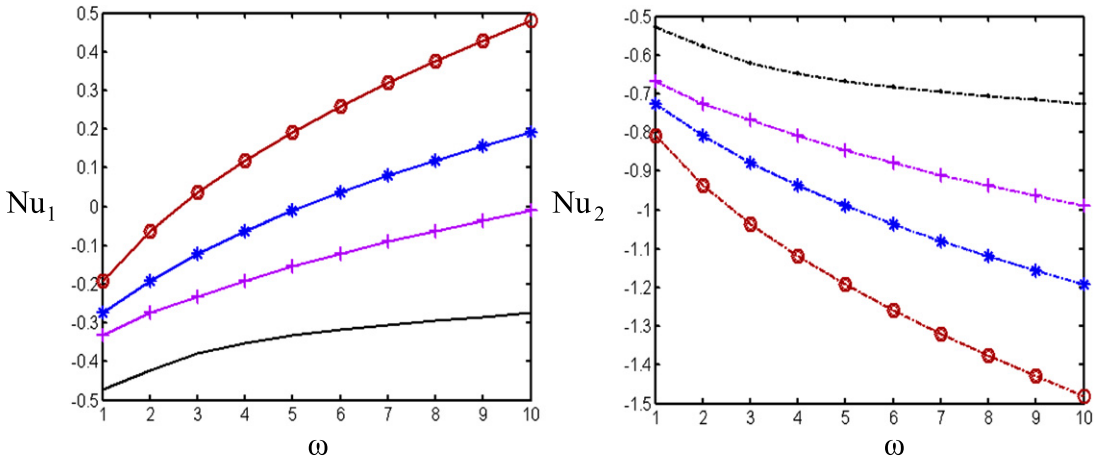

Fig. 6. Nusselt number distribution. $-S_c = 0.5, +S_c = 1, *S_c = 1.5, \circ S_c = 2$. Nu_1 – Nusselt number at the wall $y = 1, \ldots Nu_2$ – Nusselt number at the wall $y = -1$.

the first half of the channel, and gets reversed in the other half. The behavior of u_1 with changes in α is shown in Fig. 2(b). From this figure, it is clear that in the presence of heat sources ($\alpha > 0$) the fluid velocity increases from its value at $y = -1$

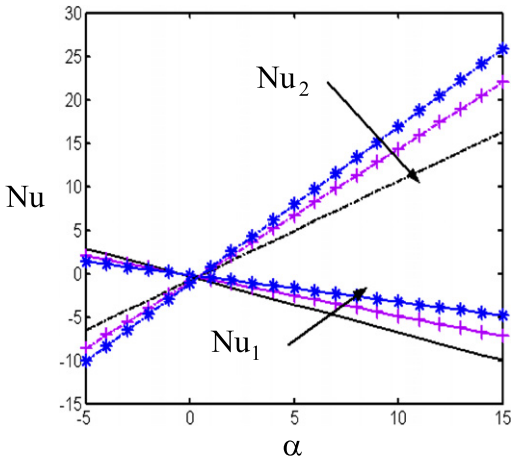

Fig. 7. Nusselt number versus α. $-P_r = 1, +P_r = 3, *P_r = 5, Nu_1$ – at the wall $y = 1, Nu_2$ – at the wall $y = -1$.

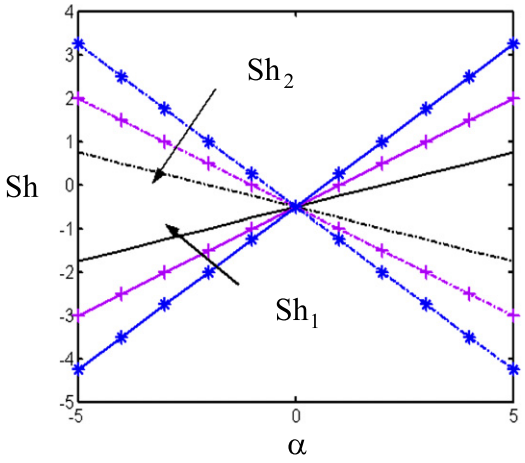

Fig. 8. Sherwood number versus α. $-S_r = 0.5, +S_r = 1, *S_r = 1.5, Sh_1$ – at the wall $y = 1, \ldots Sh_2$ – at the wall $y = -1$.

to a maximum velocity (at $y = 0.5$) then decreases steadily to its value at $y = 1$. In the presence of heat sink ($\alpha < 0$) the behavior of u_1 is exact opposite of that observed in the case of heat sources ($\alpha > 0$). From Fig. 2(c), it is evident that u_1 leads to increase in the central part of the channel ($-0.45 < y < 0.5$) with an increase in S_c. The effect of G_r on u_1 is presented in Fig. 2(d). We notice that an increase of the reversal flow with the increase of G_r. A similar result can be observed in Fig. 2(e) if G_r is replaced by G_c.

Fig. 3 depict the behavior of the cross velocity distribution (v) for different values of M, D_a, S_r, α for fixed values $\omega t = \pi/4$, $\lambda = 0.02$, $P_r = 0.73$, $G_r = 15$, $G_c = 10$, $\omega = 5$, $\lambda x = \pi/2$, $\varepsilon = 0.2$. Fig. 3(a) gives the effects of S_r on v. We see that the amplitude of v sharply increases with S_r and y near the boundaries while it decreases between these boundaries. The distribution of cross velocity for various values of α is plotted in Fig. 3(b). From this figure it is clear that in the absence of heat sources v is more like a linear function of y, while in the presence of heat sources ($\alpha > 0$) v is parabolic in nature increasing from its value at $y = -0.85$ to a maximum velocity at $y = 0$ and then decreasing steadily to its value at $y = 1$. In the presence of heat sinks ($\alpha < 0$) the behavior of v is exact opposite of that noticed in the case of heat sources (as noted in Ref. [3]). Further, Magnitude of v increases with an increase in $|\alpha|$. Fig. 3(c) describes the nature of v for different values of M at $D_a = 0.5$ and 1.5. It can be easily observed that v exhibits an oscillatory character for hydrodynamic case (as noted in Ref. [14]). Further, the cross velocity distribution is affected significantly by the magnetic field (i.e., the increasing values of M is to decrease v) while it is increases with increase of D_a. Variation of θ on v is depicted in Fig. 3(d). It can be observed that magnitude of the oscillations of v increases with the increase of θ. Further, minimum velocity drift towards the left wall and maximum velocity occurs nearer to the right wall of the vertical channel.

The total solution of temperature distribution (T) for different values of α with fixed values of $\omega t = \pi/4$, $P_r = 0.73$, $\theta = 0$, $\lambda x = \pi/2$, $\varepsilon = 0.2$, $S_r = 0.05$, $S_c = 0.005$, $\omega = 10$ is graphed in Fig. 4. From this figure, it is clear that increasing α, increases the temperature. Fig. 5 depicts that the behavior of the concentration distribution (ϕ) against y for various values of S_c with fixed values of $\omega t = \pi/4$, $P_r = 0.73$, $\theta = 0$, $\lambda x = \pi/2$, $\varepsilon = 0.2$, $S_r = 1.5$, $S_c = 1.5$, $\omega = 10$. We find that ϕ is positive and increases significantly with both S_c and y for $\alpha > 0$ but quite opposite behavior can be noticed at $\alpha < 0$.

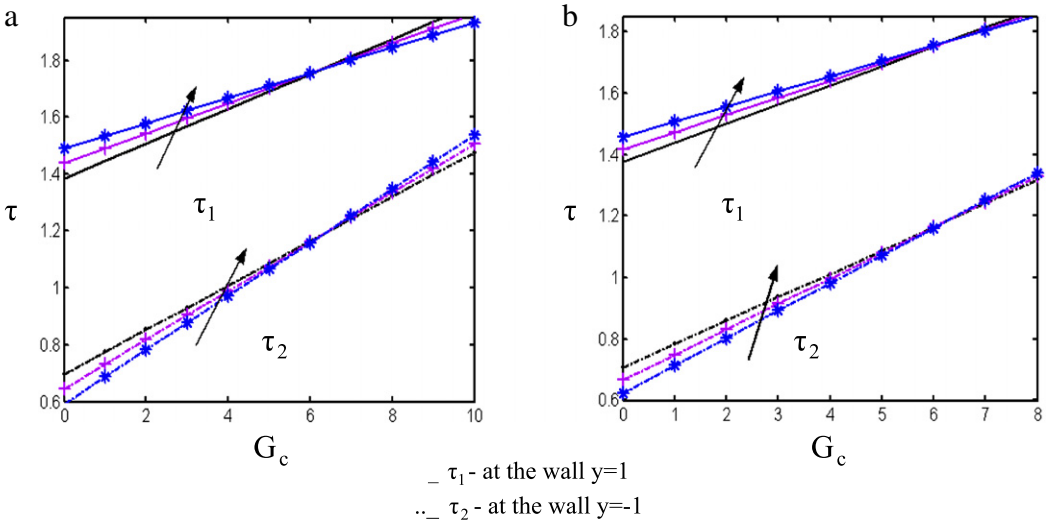

Fig. 9. Skin friction versus G_c. (a) $-S_c = 0.5, +S_c = 1, *S_c = 1.5$. (b) $S_r = 0.4, +S_r = 0.8, *S_r = 1.2$.

Fig. 6 show the variation in Nusselt number (Nu) with frequency parameter (ω) for different values of S_c with fixed values of $\omega t = \pi/4$, $P_r = 0.73$, $\theta = 0$, $\lambda x = \pi/2$, $\varepsilon = 0.2$, $\omega = 5$. We notice that Nu increases, with an increase of ω and S_c at the wall $y = 1$, but this behavior is reversed at the other wall. Fig. 7 depicts the effect of P_r on Nusselt number distribution for fixed values of $\omega t = \pi/4$, $\theta = 0$, $\lambda x = 0.02$, $\varepsilon = 0.2$, $\omega = 5$. It is noted that the presence of heat sinks, Nu_1 is positive and Nu_2 is negative, while Nu_1 is negative and Nu_2 is positive at the presence of heat source. Physically it means that the heat can some times flow out of and other times into either wall. A similar result can be observed with the respect to Sherwood number distribution, but the behavior is reversed in Fig. 8.

Fig. 9(a) displays that the effect of S_c on the skin friction versus G_c at the channel walls for constant values of $\omega t = \pi/4$, $P_r = 0.73$, $\omega = 10$, $\theta = 0$, $\lambda x = \pi/2$, $D_a = 0.5$, $\varepsilon = 0.2$. It is evident that the effect of S_c is to increase the skin friction when $0 < G_c < 6$, after which it decreases with increase of S_c at the wall $y = 1$. The reverse effect can be noticed at the other wall $y = -1$. A similar result is observed in Fig. 9(b) if S_c is replaced by S_r. Further, for a fixed value of G_c stress at the right wall ($y = 1$) is higher than that of left wall ($y = -1$).

5. Conclusions

The problem of mixed convection heat and mass transfer in a vertical wavy channel through porous medium has been analyzed. The flow is generated by the periodic thermal waves prescribed at the wavy walls of the channel. The governing equations are solved using perturbation technique subject to the relevant boundary conditions with the assumption that the solution consists of a mean part and a perturbed part. The results show that the velocity for the MHD fluid is less when compared with hydrodynamic fluid. The main flow velocity increases with the increase of D_a. The effect of Hartmann number M on the main flow velocity is quite opposite to that of D_a. The cross velocity decreases with the increase of D_a while it increases with increasing values of S_r and α. Nusselt number increases with increasing values of S_c at the wall $y = 1$ while it is decreases at the other wall and magnitude of Nusselt number increases with the increasing values of P_r. The opposite effect could be noticed in Sherwood number distribution for different values of S_r. Also, the parameters, M, D_a leads to decrease the skin friction at both the walls.

References

[1] J.H. Jang, W.M. Yan, Mixed convection heat and mass transfer along a vertical wavy surface, Int. J. Heat Mass Transfer 47 (2004) 419–428.
[2] N.T. Eldabe, M.F. El-Sayed, A.Y. Ghaly, H.M. Sayed, Mixed convective heat and mass transfer in a non-Newtonian fluid at a peristaltic surface with temperature-dependent viscosity, Arch. Appl. Mech. 78 (2008) 599–624.
[3] K. Vajravelu, Combined free and forced convection in hydromagnetic flows in Vertical wavy channels, with traveling thermal waves, Int. J. Engg. Sci. 27 (1989) 289–300.
[4] K.J. Cho, M.-U. Kim, H.D. Shin, Linear stability of two-dimensional steady flow in wavy-walled channels, Fluid Dynamics Res. 23 (1998) 349–370.
[5] A.J Chamkha, Camille Issa, Mixed convection effects on unsteady flow and heat transfer over a stretched surface, Int. Comm. Heat Mass Transfer 26 (1991) 717–727.
[6] S.D. Harris, D.B Ingham, I. Pop, Unsteady mixed convection boundary layer flow on a vertical surface in a porous medium, Int. J. Heat Mass Transfer 42 (1999) 357–372.
[7] A. Barletta, E. Zanchini, Time-periodic laminar mixed convection in an inclined channel, Int. J. Heat Mass Transfer 46 (2006) 551–563.
[8] R. Mebrouk, B. Abdellah, S. Abdelkader, B. Khadidja, Effect of wall waviness on Heat transfer by Natural convection in a Horizontal wavy enclosure, Int. J. App. Engg. Res. 1 (2006) 187–201.
[9] N.T. Eldabe, G.M. Moatimid, H.S.M. Ali, Rivlin–Ericksen fluid in tube of varying cross-section with mass and heat transfer, Z. Naturforsch. 57 (a) (2002) 863–873.

[10] A. Nield, A. Bejan, Convection in Porous Media, 2nd ed, Springer, Newyork, 1999.
[11] K. Vafai. (Ed.), Hand Book of Porous Media, vol. II, Marcel Dekker, Newyork, 2002.
[12] I. Pop, D.B. Ingham, Convective Heat Transfer: Computational and Mathematical of Modeling Viscous Fluids and Porous Media, Pergamon, Oxford, 2001.
[13] A. Bejan, A.D. Kraus, Heat Transfer Handbook, Wiley, Newyork, 2003.
[14] M. Guria, R.N. Jana, Hydrodynamic flows through vertical wavy channel with traveling thermal waves embedded in porous medium, Int. J. Appl. Mech. Engg. 3 (2006) 609–621.
[15] E.R.G. Eckert, R.M. Drake, Analysis of Heat and Mass Transfer, McGraw-Hill, New York, 1972.
[16] Z. Dursunkaya, W.M. Worek, Diffusion-thermo and thermal-diffusion effects in transient and steady natural convection from vertical surface, Int. J. Heat Mass Transfer 35 (1992) 2060–2065.
[17] A. Postelnicu, Influence of a magnetic field on heat and mass transfer by natural convection from vertical surfaces in porous media considering Soret and Dufour effects, Int. J. Heat Mass Transfer 47 (2004) 1467–1472.
[18] M.S. Alam, M.M. Rahman, M.A. Samad, Numerical study of the combined free forced convection and mass transfer flow past a vertical porous plate in a porous medium with heat generation and thermal diffusion, Nonlinear Anal.: Model. Control 11 (2006) 331–343.
[19] M.S. Malashetty, S.N. Gaikwad, M. Swamy, An analytical study of linear and non-linear double diffusive convection with Soret effect in couple stress liquids, Int. J. Thermal Sci. 45 (2006) 897–907.
[20] P.A. Lakshmi Narayana, P.V.S.N. Murthy, R.S.R. Gorla, Soret-driven thermosolutal convection induced by inclined thermal and solutal gradients in a shallow horizontal layer of a porous medium, J. Fluid Mech. 612 (2008) 1–19.
[21] S.N. Gaikwad, M.S. Malashetty, K. Rama Prasad, An analytical study of linear and nonlinear double diffusive convection in a fluid saturated anisotropic porous layer with Soret effect, Appl. Math. Model. 33 (2009) 3617–3635.
[22] S. Srinivas, M. Kothandapani, The influence of heat and mass transfer on MHD peristaltic flow through a porous space with compliant walls, Appl. Math. Comput. 213 (2009) 197–208.